

Pabst, Markus; Darnieder, Maximilian; Theska, René; Fröhlich, Thomas

Adjustment concept for compensating for stiffness and tilt sensitivity of a novel monolithic electromagnetic force compensation (EMFC) weighing cell

Original published in: Journal of sensors and sensor systems. - Göttingen : Copernicus Publ.. - 11 (2022), 1, p. 109-116.
Original published: 2022-04-07
ISSN: 2194-878X
DOI: [10.5194/jsss-11-109-2022](https://doi.org/10.5194/jsss-11-109-2022)
[Visited: 2022-04-27]



This work is licensed under a [Creative Commons Attribution 4.0 International license](https://creativecommons.org/licenses/by/4.0/). To view a copy of this license, visit <https://creativecommons.org/licenses/by/4.0/>



Adjustment concept for compensating for stiffness and tilt sensitivity of a novel monolithic electromagnetic force compensation (EMFC) weighing cell

Markus Pabst¹, Maximilian Darnieder², René Theska², and Thomas Fröhlich¹

¹Department of Mechanical Engineering, Institute of Process Measurement and Sensor Technology, Process Measurement Group, Technische Universität Ilmenau, Ilmenau, Germany

²Department of Mechanical Engineering, Institute for Design and Precision Engineering, Precision Engineering Group, Technische Universität Ilmenau, Ilmenau, Germany

Correspondence: Markus Pabst (markus.pabst@tu-ilmenau.de)

Received: 22 September 2021 – Revised: 17 February 2022 – Accepted: 25 February 2022 – Published: 7 April 2022

Abstract. This paper describes the new adjustment concept of novel planar, monolithic, high-precision electromagnetic force compensation weighing cells. The concept allows the stiffness and the tilt sensitivity of the compliant mechanisms that are dependent on the nominal load on the weighing pan to be adjusted to an optimum. The new mechanism is set up and adjusted according to the developed mechanical model. For evaluation of the concept the system is tested on a high-precision tilt table and under high vacuum conditions in the environment of a commercially available mass comparator.

1 Introduction

In 2019 the système international d'unités (SI) was redefined by the use of fundamental physical and atomic constants (Stock et al., 2019). The definition of the kilogram by the international prototype kilogram (IPK) (Quinn, 1991) was replaced by the definition through the Planck constant h (BIPM, 2019). The revised SI ensures an invariable definition of the kilogram. Nevertheless, there are uncertainty issues.

Mass comparators are commonly used for the determination of mass. The counterweight principle allows many uncertainty sources to be shortcut and the resolution of the mass determination to be significantly increased. For example, a mass comparison at a specific site in a finite period of time is nearly independent of the well-known spatial variation in gravitational acceleration.

The main component of the highly sensitive devices is an electromagnetic force compensation (EMFC) weighing cell. They are essential for recent research concerning the new definition of the kilogram (Hilbrunner et al., 2018; Fröhlich et al., 2020; Rogge and Fröhlich, 2021). Nevertheless the sensitivity of the weighing cells S is dependent on mechanical stiffness C . A large contribution to uncertainties of

the measurements with EMFC weighing cells is due to the weighing cell's sensitivity to tilt D . In the following, a concept to improve the performance of EMFC weighing cells based on mechanical adjustment is presented. The concept maximizes the sensor sensitivity from Eq. (1) by reducing the stiffness $C \rightarrow 0$, and at the same time, it minimizes the tilt sensitivity $D \rightarrow 0$, which results in a reduction of measurement uncertainties.

$$S = 1/C \quad (1)$$

2 Operating principle of EMFC weighing cells

Monolithic EMFC weighing cells consist of a parallelogram guide structure realized by the upper (3) and the lower lever (2), connected to the base (1) by flexure hinges (A) and (B) and to the load carrier (4) by flexure hinges (C) and (D), as seen in Fig. 1. An upper weighing pan (6) and a lower weighing pan (5) are connected to the load carrier (4), for different applications. Usually only one of the weighing pans is used at the same time. The coupling element (7) connects the load carrier (4) with the transmission lever (8). The transmission lever (8) transmits the force of the coun-

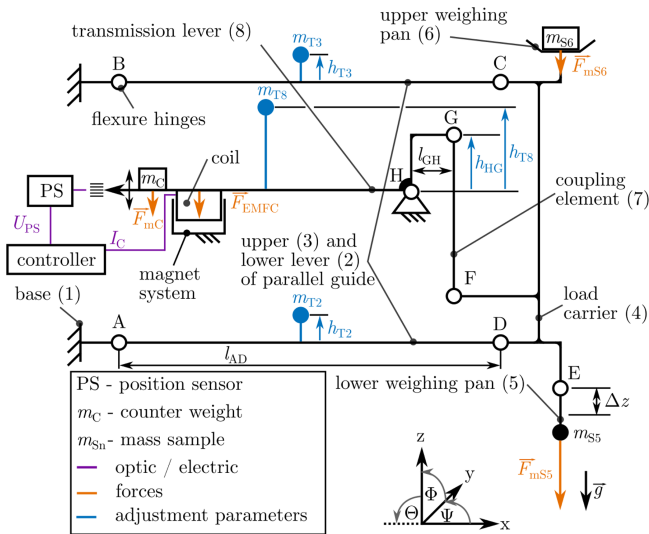


Figure 1. Operating principle of the prototype planar monolithic EMFC weighing cell with adjustment facilities (blue).

terweight $F_{mC} = m_C \cdot g$ and the electromagnetic compensation force F_{EMFC} according to the lever ratio Γ from Eq. (2) of the point of force application $l_{F_{EMFC}H}$ and l_{HG} in the x direction to compensate for the forces $F_{mS5} = m_{S5} \cdot g$ or $F_{mS6} = m_{S6} \cdot g$. Similarly, deflections Δz are transmitted to the position sensor (PS).

$$\Gamma = \frac{l_{F_{EMFC}H}}{l_{HG}} \approx 4 \tag{2}$$

The position sensor consists of an infrared-light-emitting diode and a differential photo diode, mounted face to face to the base, and a slit aperture mounted to the transmission lever. The components need to be fixed to the mechanism in its initial manufactured position, hereafter called the zero position. In the zero position, the differential photo diode and the infrared-light-emitting diode are adjusted in their position to the slit aperture at the lever until the differential voltage U_{PS} is zero. The differential voltage is obtained by transmitting the two photo currents from the differential photo diode by a transimpedance amplifier to a voltage signal. In this way the position of the lever can be detected by voltage measurements in further experiments.

In a perfect, theoretical equilibrium state, the counterweight m_C counteracts the exact mass on one of the weighing pans (m_{S5} or m_{S6}), and the weighing cell is in its zero position. In practical operation, the equilibrium state can only be reached by the application of an additional force F_{EMFC} from Eq. (3). It is a Lorentz force generated by a current carrying coil with a wire length of l in a magnetic field B . Assuming that the windings of the coil are orthogonal to the magnetic field ($B \perp I$), the coil current I_C is proportional to the generated Lorentz force (Eq. 3). With the detected deviation from the zero position by the position sensor, the coil

current is driven by a PID controller to obtain the zero position.

$$F_{EMFC} = B \cdot l \cdot I_C \tag{3}$$

Since the mechanism shown in Fig. 1 is designed in a monolithic form, all joints (A–H) are flexure hinges. Each flexure hinge has a mechanical stiffness C_{A-H} due to its geometry, thickness and material properties (Weisbord and Paros, 1965). The total mechanical stiffness of the mechanism, with all flexure hinges, is further expressed as C_{init} from Eq. (4). It describes the correlation between a differential mass Δm on one of the weighing pans in addition to mass on the weighing pan (m_{S5} or m_{S6}) and the resulting deflection Δz of the weighing pans. For further equations, it is assumed that $g \parallel z$ axis from Fig. 1.

$$C_{init.model} = f(C_{A-H}) = \frac{\Delta m \cdot g}{-\Delta z} \tag{4}$$

The calculation of the initial stiffness of the mechanism $C_{init.FEM}$ can be performed using finite element method (FEM) simulations or analytically $C_{init.model}$ with good confidence in the nominal geometry (Torres Melgarejo et al., 2018; Henning and Zentner, 2021). Deviations from the measured stiffness of prototypes are prone to manufacturing uncertainties. Even small deviations of the thickness of the hinges in the range of micrometers are critical. One way to measure C_{init} is to control the weighing cell in its zero position. Once this is achieved, the coil current I_C is kept constant, the mass m_{S6} is increased by Δm and the position Δz of the weighing pan is measured with an interferometer pointed at the weighing pan. With the mass difference Δm , the gravitational acceleration g and the deflection Δz , the stiffness can be calculated as presented in Eq. (4). The deflection at the weighing pan Δz , measured with the interferometer, is also used for the calibration of the differential voltage output of the position sensor. Once the calibration factor K_U has been determined (Eq. 5), small deflections can be measured by means of the position sensor. There is no further need for the interferometric measurement.

$$K_U = \frac{\Delta z}{\Delta U_{PS}} \tag{5}$$

Similar to the determination of the calibration factor K_U for the representation of Δz at the weighing pan, a calibration factor for the current to force correlation K_I is determined. With the controller set point for the zero position, a calibration mass Δm is placed at the weighing pan, in addition to the mass samples (m_{S5} or m_{S6}), while the coil current I_C is logged. The calculation of the calibration factor, representing the unknown parameters of the magnet system ($B \cdot l$) and the approximate lever ratio (Γ), is presented in Eq. (6).

$$K_I = \frac{B \cdot l}{\Gamma} = \frac{\Delta m \cdot g}{\Delta I_C} \tag{6}$$

The set point of the controller can be above or below the zero position, measured with the position sensor. With the mass on the weighing pan (m_{S5} or m_{S6}) kept constant while changing the set point of the controller, the stiffness can be calculated with the mass difference generated by the difference in the coil current ΔI_C , as described in Eq. (7).

$$\Delta m = \frac{\Delta I_C \cdot B \cdot l}{g \cdot \Gamma} = \frac{\Delta I_C \cdot K_I}{g} \quad (7)$$

A tilt of the base changes the direction of the force at the points of force application regarding the z axis and g . The tilt sensitivity D of EMFC weighing cells is the factor of influence by tilt to the measured mass deviation Δm_{tilt} . In the following, the tilt sensitivity is described as D_{Θ} for the tilt influences due to tilt around the y axis and D_{Φ} for the tilt sensitivity around the x axis (see Eqs. 8 and 9).

$$D_{\Theta} = \frac{\Delta m_{\text{tilt}} \cdot g}{\Delta \Theta} \quad (8)$$

$$D_{\Phi} = \frac{\Delta m_{\text{tilt}} \cdot g}{\Delta \Phi} \quad (9)$$

3 Adjustment concept

The adjustment of the EMFC weighing cell can go beyond the compensation of manufacturing and mounting deviations: it can be used to tune the mechanical properties of the weighing cell to highest sensitivity $S = 1/C$ while minimizing the tilt sensitivity D .

3.1 The auto-static state

This favorable adjustment state can be achieved by a combination of well-established adjustment methods for precision weighing systems: one method is the manipulation of trim masses m_{Tn} on bodies subject to rotary motion, e.g., the transmission lever of the weighing cell. The other measure is the introduction of a vertical distance h_{HG} between joint (H) and (G) (Darnieder et al., 2018). A perpendicular shift of a trim mass with respect to the gravitational acceleration vector g influences the static equilibrium of the balance, whereas the shift in direction of g alters stiffness and tilt sensitivity (Picard, 2004). With the stiffness, the period of free oscillations of the mechanical system is changing. In Conrady (1922), a value for the period of free oscillations was found experimentally, at which the balance is insensitive to tilt angles of its base relative to the g vector, the auto-static state. In this state, the tilt sensitivity is close to zero. Small tilts of the base, e.g., due to tidal movements of the earth's crust, do not affect the indication of the balance. Without further measures, the auto-static state of the weighing system corresponds to a certain period of free oscillations or stiffness. Consequently, the adjustment represents a trade-off between measuring sensitivity and tilt sensitivity, where the auto-static state is commonly sacrificed for a gain in measuring sensitivity (Picard, 2004).

For the typical EMFC weighing cells, this limitation can be overcome by the introduction of additional trim masses on the levers of the parallelogram guide (upper and lower lever in Fig. 1) (see also Darnieder et al., 2018, and Marangoni et al., 2017). The vertical positions of these trim masses with respect to the respective center of rotation are parametrized by h_{T2} and h_{T3} . In combination with the trim mass on the transmission lever h_{T8} , the weighing cell can be adjusted to highest sensitivity ($C \approx 0$) while maintaining zero tilt sensitivity ($D \approx 0$; auto-static state). The auto-static state is now independent of the sensitivity of the weighing cell.

3.2 Reduction of initial stiffness C_{init} by h_{HG}

Even though theoretically possible, the compensation of the entire stiffness of the weighing cell mechanism by trim masses is impractical. Either large trim masses are required, or the adjustment measures become bulky. To compensate for the biggest part of the initial stiffness, a geometry change within the mechanism can be used. Here, the relevant parameter is denoted h_{HG} – the vertical distance between the effective rotational centers of joint (H) and joint (G). The effect on the stiffness is proportional to the force flow through the coupling element (7) (Darnieder et al., 2018). In other words, the mass on the weighing pan can effectively be used as a trim mass. This advantage is a disadvantage at the same time since the sensitivity of the weighing cell becomes load-dependent. However, this is not a limiting factor for the use in a mass comparator.

To reduce the measures and masses required for the adjustment, the initial stiffness C_{init} is compensated for by h_{HG} by manufacturing according to Eq. (10). The value for the initial stiffness was calculated according to Torres Melgarejo et al. (2018) and was estimated at $C_{\text{init,model}} = 55.9 \text{ N m}^{-1}$. To compensate for the initial stiffness, the adjustment parameter h_{HG} was chosen to be 3.15 mm, which is slightly less than the calculated value for $h_{HG}(C_0 = 0)$, in order to avoid the possibility of a negative stiffness (inverted pendulum). The pre-adjusted stiffness C_0 should be close to zero but in a positive range. With $h_{HG} = 3.15 \text{ mm}$, the calculation according to Eq. (10) results in a stiffness of $C_{0,\text{calc.}} = 6.35 \text{ N m}^{-1}$. The parameter m_G is the sum of all masses suspended at joint G.

$$C_0 = C_{\text{init}} + \left(\frac{h_{HG}^2}{h_{FG}} - h_{HG} \right) m_G g l_{HG}^{-2} \quad (10)$$

3.3 Compensation of C_0 by fine-adjusting parameters

With the restriction of small rotations, applicable to EMFC weighing cells, the property variation due to an adjustment of the parameters h_{T2} , h_{T3} (further summarized as $h_{T2/T3}$) and h_{T8} can be described linearly as shown in Fig. 2. A deflection of the mechanism by Δz as well as a tilt of the base of the weighing cell will generate momentum by the trim

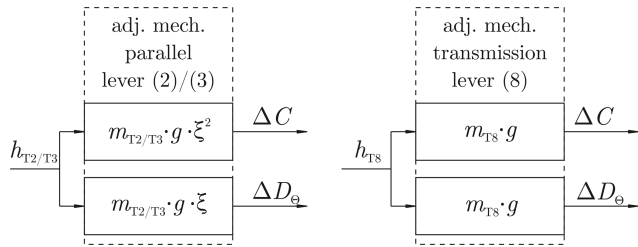


Figure 2. Linearized model equations for the adjustment of the properties stiffness C and tilt sensitivity D .

masses m_{Tn} and the measures h_{Tn} . Depending on the sign of the measures h_{Tn} , introduced momentum M_{Tn} can compensate for the tilt sensitivity as well as the stiffness. The usage of a trim mass h_{T8} on the transmission lever and the manufactured adjustment parameter h_{HG} is state-of-the-art. The introduction of the measures and trim masses on the parallel guide is new, more precisely at the upper (3) and lower lever (2). Technically, the trim masses and measures at the lower and the upper lever have the same effect, but for the assembly it is useful to use the lower lever if $h_{T2/T3} < 0$ and the upper lever if $h_{T2/T3} > 0$.

Ideally, one adjustment parameter is uniquely interrelated with one device property. As Fig. 2 shows, this is not the case. Every adjustment parameter changes both properties of interest (ΔC , ΔD). A mathematical model of the adjustment process enables a targeted adjustment. The linearized and simplified equations for both stiffness and tilt sensitivity yield ($\zeta = l_{HG}/l_{AD}$) (Darnieder et al., 2018)

$$C : 0 = C_0 l_{HG}^2 - h_{T8} m_{T8} g - (h_{T2} m_{T2} + h_{T3} m_{T3}) g \zeta^2 \quad (11)$$

$$D : 0 = D_0 l_{HG} + h_{T8} m_{T8} g + (h_{T2} m_{T2} + h_{T3} m_{T3}) g \zeta. \quad (12)$$

The values of the parameter C_0 and D_0 in Eqs. (11) and (12) need to be measured according to the measurement procedure described later in this paper with all adjustment parameters set to zero, except the manufactured h_{HG} . Given that every parameter is known except for the adjustment parameters, the equation system has one solution with $m_{T3} = 0$. The required adjustment parameters can be estimated according to Eqs. (13) and (14):

$$h_{T2/T3}^* = \frac{l_{HG}(C_0 l_{HG} + D_0)}{g m_{T2} \zeta (\zeta - 1)} \quad (13)$$

$$h_{T8}^* = -\frac{l_{HG}(C_0 l_{HG} + D_0 \zeta)}{g m_{T8} (\zeta - 1)}. \quad (14)$$

4 Measuring concept

In order to realize the adjustment process described in Fig. 3, an automatized measurement routine is needed which delivers data about the stiffness and the tilt sensitivities. Therefore

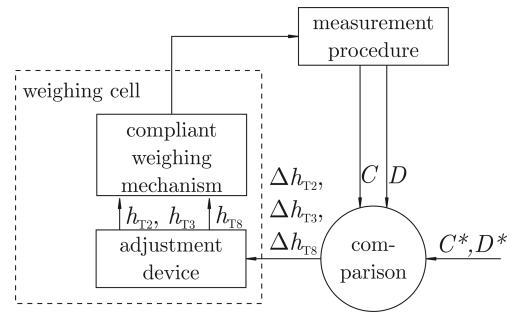


Figure 3. Adjustment process for the EMFC weighing cell. The compliant weighing mechanism and the adjustment device are part of the weighing cell.

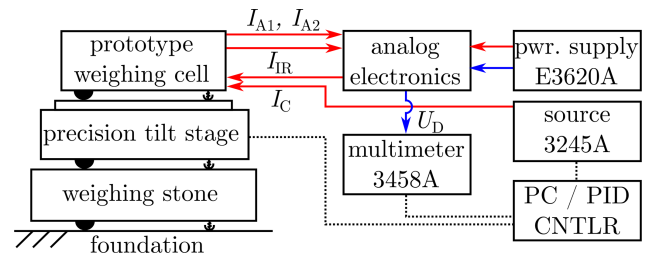


Figure 4. Schematic overview of the experimental setup with all peripheral units.

the weighing cell is placed on the high-precision tilt stage (Fig. 6), described in Rivero et al. (2014). It offers a tilt repeatability of less than $0.4 \mu\text{rad}$ in two axes (see also Yan et al., 2018, 2019). The control of the weighing cell is realized by a digital PID controller with programmable set point for the stiffness measurements. The analog electronics basically consist of a constant current supply for the infrared-light-emitting diode (I_{IR}) and a transimpedance amplifier to transform the photo currents (I_{A1} and I_{A2}) of the differential photo diode to a voltage U_{PS} (also see Fig. 4). The voltage is measured by the multimeter Agilent 3458A, which forwards the information to the computer with the digital PID controller. With the differential voltage as input, the PID controller calculates the output in terms of the coil current (I_C) which is output by the power source Agilent 3245A, connected to the coil. The control cycle reaches a frequency of 20 Hz, which is sufficient for the inert mechanical system.

During the automatized measurement routine, the tilt stage tilts the base of the weighing cell according to predefined settings. For this procedure, 27 combinations of angles of $\Theta = -15 \dots +15 \text{ mrad}$ and $\Phi = -15 \dots +15 \text{ mrad}$ were predefined. In order to counteract drifts in the signal, the position $\Theta = \Phi = 0$ was set at the beginning (step 1), in the middle (step 13) and at the end (step 27) of each measurement routine. At each position, the offset current I_C and the stiffness were measured after a defined settling time. At the end of the measurement routine, a 3D data matrix can be processed and evaluated for the stiffness, for tilt sensitivities in each

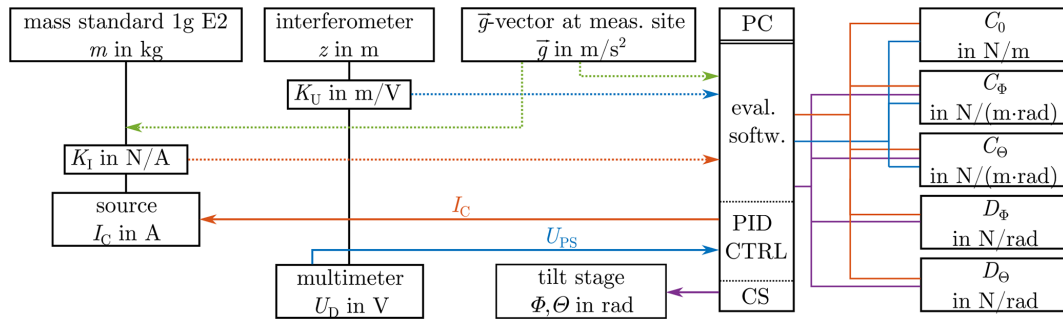


Figure 5. Information combination structure (CS – controller set point; PID CTRL – proportional integral derivative controller; PC – personal computer).

axis (D_{Θ} and D_{Φ}) and for tilt sensitivities of the stiffness itself (C_{Θ} and C_{Φ}). The obtained results can be retraced in the information combination structure in Fig. 5. The whole measurement routine has to be repeated after changing one of the adjustment parameters (m_{Tn} or h_{Tn}) or the weight on one of the weighing pans m_{Sn} , in order to investigate the influences and success of the adjustment.

5 Experimental investigations and results

For the experimental investigation, the weighing cell is set up on the precision tilt stage protected by an enclosure and a windshield to reduce the influence of air movement as shown in Fig. 6. A hood made from polystyrene covered the weighing cell during measurements to minimize the influence of temperature fluctuations. The measuring concept described above was used as the method to investigate the influences of the adjustment parameters (h_{T2} , h_{T3} , h_{T8}) in combination with the adjustment masses (m_{T2} , m_{T3} , m_{T8}) on the properties of the weighing cell concerning the stiffness and tilt sensitivities. The experiments were repeated for different loads (m_{S6}) on the weighing pan to gather information about the load dependency of the adjustment result. The momentum, M_{Tn} , described in Sect. 3, is an effective way to describe the combination of the adjustment parameters m_{Tn} with the adjustment measure h_{Tn} when divided by the gravitational acceleration, as described in Eq. (15):

$$\frac{M_{Tn}}{g} = m_{Tn} \cdot h_{Tn} \tag{15}$$

For each load, tilt sensitivities and stiffness in dependence on the adjustment state were measured. For the expression of the adjustment success A_S , the results were combined by normalizing and adding the absolute values according to Eq. (16). Since we want to compensate for the stiffness as well as the tilt sensitivity to zero, the optimum point of adjustment is at $A_S = 0$. The maximum values measured during the investigation of adjustment states with the same load of m_{S6} were used for C_{max} and $D_{\Theta,max}$. The tilt sensitivity or-

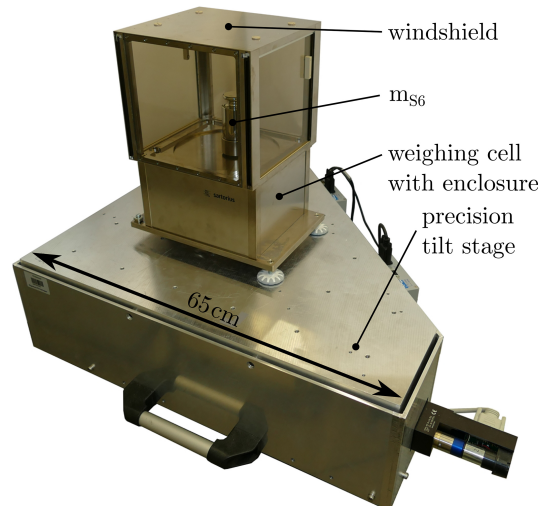


Figure 6. Prototype weighing cell in enclosure on precision tilt stage.

thogonal to the measurement direction (D_{Φ}) was not important for the adjustment success. It can not be influenced by the adjustment but delivers information about the parallelism of the axes of the tilt stage with the axes of the weighing cell.

$$A_S = \left| \frac{C_0}{C_{max}} \right| + \left| \frac{D_{\Theta}}{D_{\Theta,max}} \right| \tag{16}$$

In Figs. 7–10, the results, in terms of adjustment success, from several measurement routines for each load (m_{S6}) are presented. The black cross shows the adjustment state for the actual load, calculated from the measurement results. The black rectangle represents the area of adjustability, limited by the installation space. All combinations inside of the rectangle allow for adjustment.

Originally, the load cell was designed with $h_{HG} = 3.15$ mm for a stiffness slightly above zero. But after initial measurements with all adjustment parameters set to zero, the measured stiffness was $C_0 = -33.4$ N m⁻¹ for $m_{S6} = 1$ kg. The most likely reason for this is a deviation of thickness of

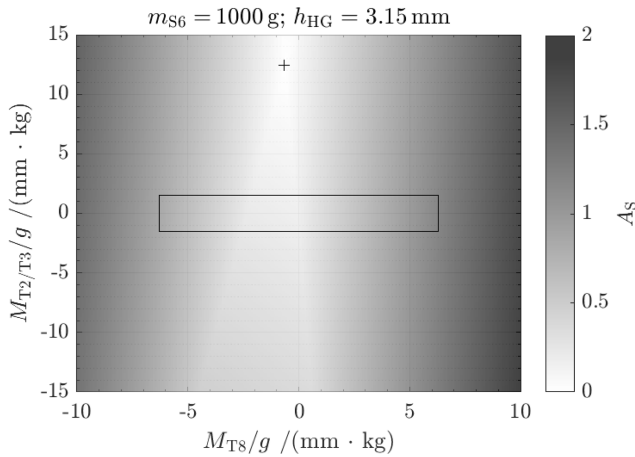


Figure 7. Adjustment success for $m_{S6} = 1000$ g.

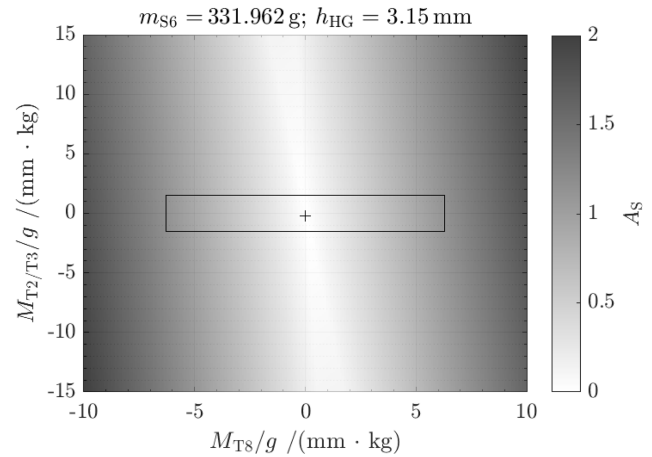


Figure 9. Adjustment success for $m_{S6} = 331.962$ g.

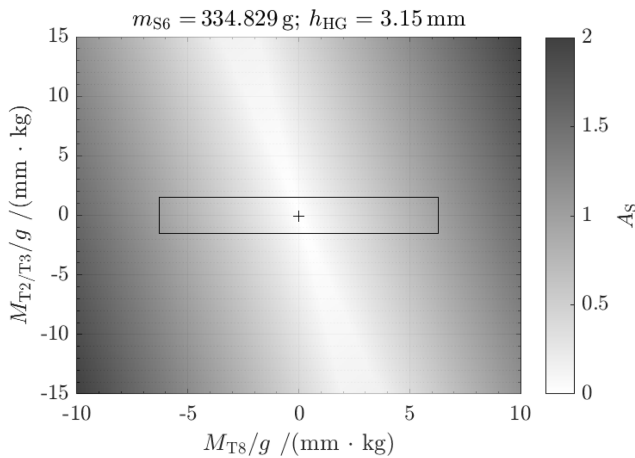


Figure 8. Adjustment success for $m_{S6} = 334.829$ g.

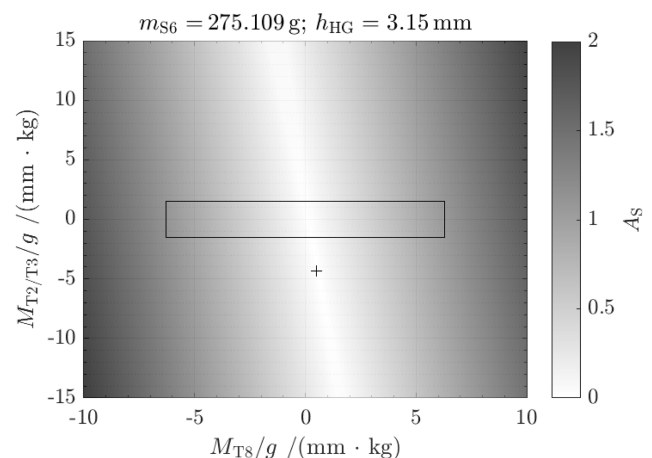


Figure 10. Adjustment success for $m_{S6} = 275.109$ g.

the flexure hinges. The thin areas are difficult to manufacture, and deviations of only a few micrometers result in significant deviations (for more information on the calculation of stiffness of flexure hinges, see Torres Melgarejo et al., 2018). According to Fig. 7, the adjustment measures for $h_{T2/T3}$ could not be reached in this case. Nevertheless, in order to provide basic evidence for the correctness of the adjustment approach, the mass of the sample on the weighing pan was reduced to about 335 g (Fig. 8). For this, a stiffness close to zero and a tilt sensitivity in the range of adjustability are achieved. This state is further called the pre-adjusted state. Several measurements were performed with varying values for h_{T8} and $h_{T2/T3}$, while the trim weights m_{T8} and $m_{T2/T3}$ were kept constant. With the measurement results, the adjustment measures were calculated for the fine-adjusted state: $h_{T2/T3} = -12.663$ mm and $h_{T8} = 0.006$ mm.

With the adjustment measures set to the weighing cell, the measurement procedure was repeated several times to obtain information about the repeatability. The results are presented in Tables 1 and 2 (fine-adjusted state). For the proof of vac-

uum compatibility, the measurements of the stiffness were repeated under high vacuum conditions ($p < 1 \times 10^{-5}$ mbar) in the environment of a high vacuum mass comparator. The results of the repeated stiffness measurements under high vacuum conditions are presented in Table 1, and the results of the milestones during the adjustment procedure are presented in Tables 1 and 2.

6 Conclusions

A novel planar monolithic electromagnetic force compensation weighing cell was manufactured and investigated. The mechanical properties of the new weighing cell can be adjusted, which allows the stiffness and the tilt sensitivity to be compensated for in a more sophisticated way.

The verification of the adjustment approach was confirmed experimentally. The initially measured stiffness was compensated for to $< 1.1\%$ in the pre-adjusted state and further reduced by 1/5 in the fine adjusted state. The tilt sensitivity

Table 1. Adjustment success for stiffness.

Properties	C in mNm^{-1}
Theoretical initial stiffness from Eq. (4): $C_{\text{init,model}}$	55 885.1
Calculated initial stiffness from Eq. (10): C_{init}	12484.1 ± 34.9
Init. meas. stiffness C_0 with $m_{S6} = 1 \text{ kg}$; $h_{HG} = 3.15 \text{ mm}$	-33420.1 ± 34.9
Pre-adjusted state C_0 with $m_{S6} = 335 \text{ g}$ and $h_{HG} = 3.15 \text{ mm}$	$-33.5 \pm 584.5^*$
Fine-adjusted state C_0 with $h_{T2/T3} = -12.663 \text{ mm}$; $h_{T8} = 0.006 \text{ mm}$	6.8 ± 52.1
Fine-adjusted state under high vacuum condition C_0 at ($p < 1 \times 10^{-5} \text{ mbar}$)	5.1 ± 12.5

Standard deviations $k = 1$. * High standard deviation is caused by the instable condition of the weighing cell with negative stiffness (inverted pendulum).

Table 2. Adjustment success for tilt sensitivity.

Properties	D_{Θ} in mNrad^{-1}
Initial tilt sensitivity D_{Θ} with $m_{S6} = 1 \text{ kg}$; $h_{HG} = 3.15 \text{ mm}$	89.662 ± 0.040
Pre-adjusted state D_{Θ} with $m_{S6} = 335 \text{ g}$ and $h_{HG} = 3.15 \text{ mm}$	5.511 ± 0.002
Fine-adjusted state D_{Θ} with $h_{T2/T3} = -12.663 \text{ mm}$; $h_{T8} = 0.006 \text{ mm}$	-0.109 ± 0.040

Standard deviations $k = 1$.

was compensated for to $< 1.3\%$ compared to the initial measured tilt sensitivity or $< 2\%$ compared to the pre-adjusted state. The vacuum compatibility of the new mechanism was confirmed for further investigations in the environment of a vacuum mass comparator. Here, the performance of the system will be determined and compared to other systems. The knowledge about the manufacturing deviations in the weighing cell will be used for further investigation and the design of the next prototype. A further improvement can be achieved by the integration of an adjustment of the parameter h_{HG} in the mechanical structure. Thereby the influence of the load as trim mass itself can be counteracted, and the weighing cell can be adapted to a wide range of loads.

Code and data availability. The underlying measurement data and software codes are not publicly available and can be requested from the authors if required.

Author contributions. MP and MD wrote the initial draft of the paper. MD was mainly involved in the modeling of the operating principle and the adjustment concept. MP was responsible for the measurement strategy, including operation of the measurements and data evaluation. RT and TF were in charge of the research concept, raised the funds and were involved in reviewing and editing of the paper.

Competing interests. At least one of the (co-)authors is a member of the editorial board of *Journal of Sensors and Sensor Systems*. The peer-review process was guided by an independent editor, and the authors also have no other competing interests to declare.

Disclaimer. Publisher's note: Copernicus Publications remains neutral with regard to jurisdictional claims in published maps and institutional affiliations.

Special issue statement. This article is part of the special issue "Sensors and Measurement Science International SMSI 2021". It is a result of the Sensor and Measurement Science International, 3–6 May 2021.

Acknowledgements. The authors would like to thank the German Research Foundation (DFG) for the financial support of the project.

Financial support. This research has been supported by the Deutsche Forschungsgemeinschaft (grant nos. TH845/7-2 and FR2779/6-2).

Review statement. This paper was edited by Andreas König and reviewed by three anonymous referees.

References

- BIPM: Le Système international d'unités/The International System of Units ("The SI Brochure"), Bureau international des poids et mesures, 9th edn., http://www.bipm.org/en/si/si_brochure/ (last access: 29 March 2022), 2019.
- Conrady, A.: A study of the balance, P. R. Soc. Lond. A-Conta., 101, 211–224, 1922.
- Darnieder, M., Pabst, M., Wenig, R., Zentner, L., Theska, R., and Fröhlich, T.: Static behavior of weighing cells, J. Sens. Syst., 7, 587–600, <https://doi.org/10.5194/jsss-7-587-2018>, 2018.
- Fröhlich, T., Rogge, N., Vasilyan, S., Rothleitner, C., Günther, L., Lin, S., Hilbrunner, F., Knopf, D., Härtig, F., and Marangoni, R.: Neue Wege zur Kalibrierung von E2-Massenormalen und Darstellung von Kräften bis 10 N, tm-Technisches Messen, 87, 280–293, <https://doi.org/10.1515/teme-2019-0143>, 2020.

- Henning, S. and Zentner, L.: Analysis of planar compliant mechanisms based on non-linear analytical modeling including shear and lateral contraction, *Mech. Mach. Theory*, 164, 104397, <https://doi.org/10.1016/j.mechmachtheory.2021.104397>, 2021.
- Hilbrunner, F., Rahneberg, I., and Fröhlich, T.: Wattwaage mit Hebelübersetzung auf Basis eines kommerziellen EMK-Wägesystems, *tm-Technisches Messen*, 85, 658–679, <https://doi.org/10.1515/teme-2017-0065>, 2018.
- Marangoni, R. R., Rahneberg, I., Hilbrunner, F., Theska, R., and Fröhlich, T.: Analysis of weighing cells based on the principle of electromagnetic force compensation, *Meas. Sci. Technol.*, 28, 075101, <https://doi.org/10.1088/1361-6501/aa6bcd>, 2017.
- Picard, A.: The BIPM flexure-strip balance FB-2, *Metrologia*, 41, 319, 2004.
- Quinn, T.: The kilogram: the present state of our knowledge, *IEEE T. Instrum. Meas.*, 40, 81–85, <https://doi.org/10.1109/tim.1990.1032888>, 1991.
- Rivero, M., Kühnel, M., and Fröhlich, T.: High precision dual axis tilt stage, in: *Proceedings of the 58th Ilmenau Scientific Colloquium, Ilmenau, 8–12 September 2014*, urn:nbn:gbv:ilm1-2014iwk:3, 2014.
- Rogge, N. and Fröhlich, T.: Nutzung eines kommerziellen EMK-Systems als Bestandteil einer Kibble-Waage, *tm-Technisches Messen*, 88, s8–s13, <https://doi.org/10.1515/teme-2021-0053>, 2021.
- Stock, M., Davis, R., de Mirandés, E., and Milton, M. J. T.: The revision of the SI – the result of three decades of progress in metrology, *Metrologia*, 56, 022001, <https://doi.org/10.1088/1681-7575/ab0013>, 2019.
- Torres Melgarejo, M. A., Darnieder, M., Linß, S., Zentner, L., Fröhlich, T., and Theska, R.: On Modeling the Bending Stiffness of Thin Semi-Circular Flexure Hinges for Precision Applications, *Actuators*, 7, 86, <https://doi.org/10.3390/act7040086>, 2018.
- Weisbord, L. and Paros, J.: How to design flexure hinges, *Mach. Des.*, 27, 151–157, 1965.
- Yan, N., Kühnel, M., Vasilyan, S., and Fröhlich, T.: Torsion balance-based system for high-precision force measurement in horizontal plane: part I. Development concept, *Meas. Sci. Technol.*, 29, 084001, <https://doi.org/10.1088/1361-6501/AABA1F>, 2018.
- Yan, N., Vasilyan, S., and Fröhlich, T.: Torsion balance-based system for high-precision force measurement in horizontal plane: part II. Static and dynamic improvement, *Meas. Sci. Technol.*, 30, 055104, <https://doi.org/10.1088/1361-6501/AB05AA>, 2019.